Title

Extrathymic Aire-Expressing Cells Are a Distinct Bone Marrow-Derived Population that Induce Functional Inactivation of CD4+ T Cells

Journal

Immunity, 39(3)

ISSN

1074-7613

Authors

Gardner, James M
Metzger, Todd C
McMahon, Eileen J
et al.

Publication Date

2013-09-01

DOI

10.1016/j.immuni.2013.08.005

Peer reviewed

Published in final edited form as:
Immunity. 2013 September 19; 39(3): 560–572. doi:10.1016/j.immuni.2013.08.005.

Extrathymic *Aire*-Expressing Cells are a Distinct Bone Marrow-Derived Population that Induce Functional Inactivation of CD4+ T Cells

James M. Gardner[1,2,*], **Todd C. Metzger**[1,*], **Eileen J. McMahon**[1,3], **Byron B. Au-Yeung**[4], **Anna K. Krawisz**[1], **Wen Lu**[1], **Jeffrey D. Price**[5], **Kellsey P. Johannes**[1], **Ansuman T. Satpathy**[6], **Kenneth M. Murphy**[6], **Kristin V. Tarbell**[5], **Arthur Weiss**[4], and **Mark S. Anderson**[1]

[1]Diabetes Center, University of California-San Francisco, San Francisco, CA 94143-0540, USA

[2]Department of Surgery, University of California-San Francisco, San Francisco, CA 94143-0540, USA

[3]Department of Biology, Westmont College, Santa Barbara, CA 93108, USA

[4]Howard Hughes Medical Institute, Rosalind Russell Medical Research Center for Arthritis, Department of Medicine, Department of Microbiology and Immunology, University of California-San Francisco, San Francisco, California, 94143-0540, USA

[5]Immune Tolerance Section, Diabetes Branch, National Institute of Diabetes and Digestive and Kidney Diseases, National Institutes of Health, Bethesda MD 20892, USA

[6]Howard Hughes Medical Institute, Department of Pathology and Immunology, School of Medicine, Washington University in St. Louis, St. Louis, MO 63110

Summary

The autoimmune regulator (*AIRE*) is essential for prevention of autoimmunity; its role is best understood in the thymus where it promotes self-tolerance through tissue-specific antigen (TSA) expression. Recently, extrathymic *Aire*-expressing cells (eTACs) have been described in murine secondary lymphoid organs, but the identity of such cells and their role in immune tolerance remains unclear. Here we have shown that eTACs are a discrete major histocompatibility complex class II (MHC II)^{hi}, CD80^{lo}, CD86^{lo}, epithelial cell adhesion molecule (EpCAM)^{hi}, CD45^{lo} bone marrow-derived peripheral antigen presenting cell (APC) population. We also have demonstrated that eTACs can functionally inactivate CD4^{+} T cells through a mechanism that does not require regulatory T cells (Treg), and is resistant to innate inflammatory stimuli. Together these findings further define eTACs as a distinct tolerogenic cell population in secondary lymphoid organs.

Introduction

Clonal diversity within the adaptive immune system allows responsiveness to a wide range of pathogens, but can also predispose to autoimmunity in the absence of appropriate self-

Correspondence: manderson@diabetes.ucsf.edu; ph. (415) 502-8052, fax (415) 564-5813.
*These authors contributed equally

The authors declare no competing financial interests.

tolerance. Education of developing T cells in the thymus is a critical component of such tolerance, and involves removal of developing autoreactive T cells (Anderson et al., 2005; Metzger and Anderson, 2011) in part through the activity of *AIRE. AIRE* was first identified in humans by positional cloning as the defective gene in the monogenic autosomal-recessive Autoimmune Polyglandular Syndrome Type I (APSI; (Nagamine et al., 1997), and *Aire*$^{-/-}$ mice develop severe, pleiotropic, multi-organ autoimmunity (Anderson et al., 2002). Thymic *Aire* expression prevents autoimmunity by exposing developing T cells in the thymus to otherwise tissue-specific antigens (TSAs) like insulin (pancreas; (Anderson et al., 2005; Derbinski et al., 2001) and vomeromodulin (lung; (Shum et al., 2009), which are transcribed in specialized *Aire*-expressing medullary thymic epithelial cells (mTECs); exposure to such antigens induces central T cell tolerance to the peripheral organs in which these antigens are normally expressed.

Aire expression has also recently been described in a population of extrathymic *Aire*-expressing cells (eTACs) in murine peripheral lymphoid organs. These cells express unique, Aire-regulated TSAs distinct from those driven by thymic Aire, and can cause activation-induced cell death of interacting CD8$^+$ T cells (Gardner et al., 2008). Other cell populations in the periphery have also been suggested to promote self-tolerance through intrinsic expression of TSAs (Cohen et al., 2010; Fletcher et al., 2010) and TSA expression in non-obese diabetic (NOD) mice lymph nodes was recently suggested to correlate with diabetes progression (Yip et al., 2009).

Despite this accumulating evidence of peripheral expression of both *Aire* and diverse TSAs, there are conflicting reports on the exact identity of the *Aire*-expressing population in the periphery. *AIRE* transcript has been found in human lymph nodes (Nagamine et al., 1997) and has also been detected at the protein level (Poliani et al., 2010). Investigations into *Aire* expression in mice have also identified *Aire* transcripts in secondary lymphoid organs, but detection of Aire protein in these tissues has been variable (Anderson et al., 2002; Halonen et al., 2001; Heino et al., 2000; Hubert et al., 2008). Also, the type of cell expressing AIRE in the periphery has been controversial, with groups reporting AIRE in both the hematopoietic and stromal lineages (Fletcher et al., 2010; Gardner et al., 2008; Poliani et al., 2010).

Previously, we showed that eTACs express high amounts of major histocompatibility complex class II (MHC II) and relevant antigen processing machinery, but lack the high expression of CD80 and CD86 that characterize other antigen presenting cell (APC) populations (Gardner et al., 2008). While low expression of CD80 and CD86 has also been described for other peripheral TSA-expressing populations (Lukacs-Kornek et al., 2011), these cells appear to express minimal MHC II in the absence of inflammatory signals (Malhotra et al., 2012). Nevertheless, the ability of any peripheral TSA-expressing population to interact with CD4$^+$ T cells or affect the development of autoimmune disease has remained unclear.

Here we have identified eTACs as a distinct CD45^{lo} bone marrow-derived APC population, thus reconciling conflicting reports about the identity of eTACs. We also found that targeted expression of pancreatic antigens in eTACs robustly prevented CD4$^+$ T cell-mediated autoimmune diabetes. We demonstrated that such tolerance induction was highly resistant to conversion from tolerance to immunogenicity and persisted upon serial transfer to susceptible secondary hosts. Finally, we have shown that the mechanism of eTAC-mediated tolerance depends primarily on the induction of functional inactivation among effectors and not on regulatory T cell (Treg) enrichment, and does so through a mechanism involving deficient costimulation. Together, these results identify eTACs as a discrete, unique population of bone marrow-derived tolerogenic APCs.

Results

Murine eTACs are a distinct bone marrow-derived APC population

Recent evidence suggests that peripheral *Aire* expression maps to a radioresistant cell population (Fletcher et al., 2010; Gardner et al., 2008) but a lack of clarity on markers expressed on eTACs has hindered direct analysis of these cells. Utilizing our previously described Aire-reporter mouse (Adig) in which Aire drives expression of GFP and the islet-specific glucose-6-phosphatase-related protein (IGRP) antigen (Gardner et al., 2008), we sought to more precisely define this cell population. To map the origin of these cells, we first generated reciprocal bone marrow chimeras and examined the ability of Aire-driven antigen to induce proliferation of transferred IGRP-specific T cells. Consistent with our previous work, we observed that radioresistant cells drove T cell proliferation (Figure 1A), but also found strong evidence for increased proliferation in wildtype (WT) recipients of Adig bone marrow, suggesting that eTACs may be a bone marrow-derived but partially radioresistant population. Importantly, while residual radioresistant eTACs were sufficient to induce *8.*3 T cell deletion as we reported previously (Gardner et al., 2008), eTACs recently generated from the bone marrow were also capable of deleting *8.*3 T cells (Figure S1A). We next examined peripheral lymphoid organs of these reciprocal chimeric mice, and observed that the vast majority of GFP^+ $CD45^{lo}$ $MHCII^+$ eTACs were in fact derived from the bone marrow compartment (Figure 1B), and nuclear Aire staining colocalized with GFP only when the *Aire*-GFP transgene was expressed by bone marrow-derived cells (Figure 1C). However, we did occasionally observe residual *Aire*-GFP^+ eTACs in transgenic mice receiving WT bone marrow (Figure S1B), consistent with prior identification of some radioresistance by eTACs (Gardner et al., 2008). Together, these results demonstrate that eTACs represent a radioresistant bone marrow-derived and not a stromal lineage.

We next revisited expression of the pan-hematopoietic marker CD45 on eTACs. Through the use of additional markers such as epithelial cell adhesion marker (EpCAM) and CD86, we found that eTACs were not strictly negative for CD45, as reported previously population (Fletcher et al., 2010; Gardner et al., 2008), but rather expressed low amounts of CD45 (Figure 2A, 2B, S2A). Interestingly, we analyzed the appearance of eTACs on the stromal cell gating strategy used previously (Fletcher et al., 2010) to identify *Aire* message among $gp38^-$ $CD31^-$ $CD45^{lo}$ events, and found that eTACs likely fell within this gate due to low but non-negative CD45 expression (Figure 2C, 2D). This likely explains previous reports of *Aire* message being detectable in $CD45^-$ populations, and definitively establishes eTACs as a bone marrow-derived population.

We next sorted eTACs for comparison to $Aire^+$ mTECs and conventional DCs (cDC), two APC populations with similar transcriptional profiles to eTACs (Gardner et al., 2008), and found that while TSA and Aire expression were highly restricted to eTACs and mTECs, eTACs exhibited low expression of the characteristic DC markers CD45 and CD11c (Figure 2B). Importantly, eTACs and DCs had comparable expression of Zbtb46, a recently identified marker of the classical DC lineage (Satpathy et al., 2012) (Figure 2B). We also examined eTACs from Zbtb46 reporter mice and found equivalent GFP expression in eTACs and cDCs (Figure 2E). In contrast to DCs, eTACs only weakly expressed CD80 and CD86 by qPCR (Figure 2F), and lacked expression of most Fc receptors examined (Figure S2B), suggesting a limited potential internalize and present opsonized foreign antigen. Of note, eTACs and DCs both expressed Deaf-1, (Figure 2F), although the transcriptional variant of Deaf-1 that Yip et al. associated with TSA expression was undetectable in sorted cell populations (2009). Finally, sorted eTACs also displayed cDC-like morphological features, namely a large, highly vacuolated cytoplasm (Figure 2G). To further characterize the relationship of cDCs and eTACs, we examined a panel of surface markers characteristic

of cDCs (Figure 2H) and plasmacytoid DCs (Figure S2C), and found that eTACs fell into neither group, and appeared to represent a distinct, non-conventional APC population.

eTACs are present in human secondary lymphoid organs

To identify and characterize peripheral *AIRE*-expressing populations in humans, we examined lymph node sections by immunofluorescence and were able to identify discrete cells expressing intranuclear AIRE protein (Figure 3A) in all patient samples examined (6/6). Further, as in mouse, human eTACs were uniformly MHC II$^+$, and localized to the subcapsular zone at the boundary between the T cell paracortex and B cell follicles within the lymph node (Figure 3A). Importantly, we found that AIRE protein in human eTACs and mTECs was exclusively intranuclear and concentrated in nuclear speckles (Figure 3B, S3A, S3B), similar to the localization of transcriptionally active AIRE protein in the thymus (Su et al., 2008). As in mice (Gardner et al., 2008) (Figure 2), human eTACs did not stain strongly for the conventional DC markers CD11c and CD45, and also lacked CD11b (Figure 3C). Together, these results identify a discrete population of eTACs in human secondary lymphoid organs closely resembling their murine counterparts.

Transgenic *Aire*-driven BDC peptide is expressed in mTECs and eTACs

Given the high expression of MHC II by mouse and human eTACs, we hypothesized that eTACs might interact with CD4$^+$ T cells. To investigate this we turned to the BDC2.5 TCR-transgenic mouse model of diabetes (Katz et al., 1993), in which diabetogenic CD4$^+$ T cells react to a pancreatic antigen derived from chromogranin A (Stadinski et al., 2010), as well as its mimetope peptide p31 (Judkowski et al., 2001). By inserting the BDC mimetope peptide into the MHC class II molecule-associated invariant Chain (Ii or CD74) under direction of the Aire promoter (van Santen et al., 2004), we were able to direct presentation of p31 and expression of GFP to mTECs and eTACs in an *Aire*-driven BDC antigen (AdBDC) transgenic mouse (Figure 4A). Localization of mTECs and eTACs to the thymic medulla and boundary of the T and B cell zones, respectively, was confirmed, as was colabeling of *Aire*-expressing cells with both Aire protein and GFP (Figure 4B). Examination of surface marker expression on GFP$^+$ cells from Adig and AdBDC mice confirmed that *Aire*-expressing cells identified by the two reporters had identical profiles (Figure 4C, 4D). Together, these results demonstrate that the AdBDC transgene faithfully recapitulates endogenous *Aire* expression in mTECs and eTACs.

eTACs interact with cognate CD4$^+$ T cells and drive tolerance in *AdBDC* mice

To test whether eTACs could present antigen to CD4$^+$ T cells, we performed adoptive transfers of congenically-marked, CFSE-labeled BDC2.5 CD4$^+$ T cells. Three days post-transfer, BDC2.5 T cells were found to proliferate only in the pancreatic lymph nodes in WT recipients. In contrast, robust proliferation of BDC2.5 T cells was observed in all secondary lymphoid organs of AdBDC mice, and by two weeks post-transfer, notable residual populations remained which had completely diluted CFSE (Figure 5A). Importantly, proliferation was also observed in AdBDC mice reconstituted with MHCII deficient bone marrow (Figure S4A), demonstrating that that direct antigen presentation by radioresistant eTACs (Figure S1B) was sufficient to drive BDC2.5 T cell proliferation.

We next tested whether cognate antigen expression in eTACs could directly impact BDC2.5-mediated autoimmune diabetes. Purified populations of naïve, CD25-depleted BDC2.5 T cells rapidly cause diabetes in NOD severe combined immunodeficiency (SCID) hosts after adoptive transfer (Figure 5B). However, cognate antigen expression on host eTACs in AdBDC SCID recipients led to complete protection from BDC2.5-mediated diabetes and prevention of islet infiltration (Figure 5B, 5C), suggesting that proliferating

BDC2.5 T cells in AdBDC SCID recipients died or remained functionally sequestered prior to reaching the target tissue.

We next addressed whether such tolerogenic function was a non-specific result of antigen presentation by any non-inflammatory APC. To accomplish this we covalently conjugated BDC2.5 mimetope antigen to an anti-DEC205 antibody (DEC1040), which leads to presentation of the conjugated antigen by tolerogenic DEC205$^+$ DCs (Bonifaz et al., 2002). Although this method of delivery differed from the transgenic approach used in AdBDC eTACs, DEC1040-mediated loading of DCs induced robust proliferation of cognate BDC2.5 T cells (Figure S4B). However, such BDC2.5 T cell-DC interactions in DEC1040-treated NOD SCID recipients failed to prevent or slow progression of BDC2.5-mediated autoimmune diabetes (Figure 5B). Together, these data indicate that antigen-specific eTAC-CD4$^+$ interactions lead to rapid proliferation and subsequent inactivation of interacting T cells, and result in complete protection from both insulitis and autoimmune diabetes.

eTAC interaction leads to Treg cell enrichment, but tolerance is Treg cell-independent

We next attempted to investigate the mechanism of such tolerance by characterizing the phenotype and function of residual eTAC-experienced CD4$^+$ T cells in AdBDC hosts (Figure 5A). Despite prolonged interaction with antigen-bearing eTACs, residual BDC2.5 T cells retained avidity for I-Ag7-p31 tetramer (Figure 6A), suggesting that the surviving T cells in this context had not lost their antigen-specificity or undergone T cell receptor (TCR) downregulation. These residual BDC2.5 T cells were enriched for Foxp3$^+$ Treg cells (Figure 6B, 6C) despite pre-transfer CD25 depletion, and enrichment was most prominent in non-antigen draining sites, suggesting eTAC interactions in the absence of competing APC populations may favor the preferential expansion, retention, or survival of Treg cells.

To determine whether this peripheral Treg cell expansion and enrichment explained the mechanism of tolerance induced by eTACs, we next crossed BDC2.5 TCR-transgenic mice with NOD Foxp3-diphtheria toxin receptor (DTR) transgenic mice, which rapidly deplete Foxp3$^+$ Treg cells upon exposure to diphtheria toxin (Feuerer et al., 2009) (Figure S5A). We adoptively transferred BDC2.5$^+$ Foxp3-DTR$^+$ T cells into WT or AdBDC SCID mice treated continuously with diphtheria toxin and found that while WT SCID hosts progressed rapidly to diabetes, AdBDC SCID recipients remained disease-free (Figure 6D). Furthermore, the islets of AdBDC SCID hosts remained devoid of T cell infiltrates, demonstrating the inability of eTAC-experienced BDC2.5 effector T cells to reach the target organ even in the absence of Treg cells (Figure S5B). These results suggest that while eTAC-CD4$^+$ T cell interactions support the enrichment of Treg cells, such regulatory populations are not required for eTAC-mediated tolerance.

As the activity of Treg cells in *trans* was not critical for eTAC-mediated tolerance of BDC2.5 T cells, we next explored whether effector T cells might be functionally inactivated in *cis* with a serial co-transfer system. Ten days after adoptive transfer of CD25-depleted BDC2.5 T cells into WT and AdBDC SCID hosts, lymphocytes were harvested, purified, and re-transferred into secondary WT lymphopenic recipients either alone or mixed 1:1 with freshly isolated naïve, CD25-depleted BDC2.5 T cells (Figure 6E). BDC2.5 lymphocytes serially transferred from WT SCID mice again induced diabetes in secondary SCID hosts, while serially transferred lymphocytes from AdBDC SCID mice still failed to induce diabetes, despite the absence of continued exposure to cognate antigen-loaded eTACs (Figure 6F). Consistent with the results of the Foxp3-DTR experiments above, BDC2.5 T cells harvested from either WT or AdBDC SCID hosts did not mediate tolerance in *trans*, as serial co-transfer of purified CD4$^+$ lymphocytes mixed 1:1 with freshly isolated naïve BDC2.5 T cells failed to suppress or delay disease onset (Figure 6F). Together, these data

suggest that eTAC-mediated tolerance operates primarily in *cis*—via induction of functional inactivation of effectors—and not in *trans*—via expansion of Treg cells.

eTAC-CD4$^+$ T cell interaction induces functional inactivation via absence of costimulatory signals

To further examine effector T cell inactivation following eTAC encounter, we characterized tolerized BDC2.5 T cells following transfer to AdBDC hosts. Consistent with functional inactivation of effectors, we observed that tolerized T cells expressed high amounts of programmed cell death 1 (PD-1) and the tolerance-associated markers CD73, FR4, and Lag3 (Bettini et al., 2011; Martinez et al., 2012), and also had diminished interleukin-2 (IL-2) production (Figure S5C–F). Next, we adoptively transferred naïve BDC2.5 T cells into AdBDC and WT mice, immunized these recipients at day 14 post-transfer with p31 and adjuvant, and measured interferon-γ (IFN-γ) production three days later (Figure 7A). Whereas BDC2.5 T cells isolated from WT hosts retained the ability to produce IFN-γ after immunization, BDC2.5 T cells from AdBDC mice remained unresponsive (Figure 7B). Likewise, and consistent with the disease transfer results described above, pretreatment of recipient mice with DEC205$^+$ DC-targeted antigen failed to induce anergy upon rechallenge, and indeed led to a more robust secondary recall response (Figure 7B), further suggesting that eTACs induce anergy through a cell-type specific mechanism.

To further delineate the mechanisms of eTAC-mediated tolerance, we next interrogated a broad range of established tolerogenic pathways. Notably, blockade of other established inhibitory pathways including programmed cell death ligand 1 (PD-L1) and interleukin-10 (IL-10) failed to break eTAC-mediated tolerance (Figure S6A–C). Likewise, we investigated the OX40 alternative costimulatory pathway, which is able to override tolerance in some situations (Lathrop et al., 2004). OX40 was upregulated on BDC2.5 T cells shortly after eTAC encounter (Figure S6D) and provision of agonist signal through this receptor could drive an activated phenotype in otherwise tolerized BDC2.5 T cells (Figure S6E), although signaling through this pathway was similarly unable to override the diabetes protection observed in AdBDC SCID mice (Figure S6F). Because strong costimulation through OX40 engagement could partially override tolerance, we next explored the possibility that the paucity of B7 costimulation on eTACs contributed to their tolerogenic activity (Harding et al., 1992). First, we addressed whether low CD80 expression by eTACs was sensitive to inflammatory signals, and found that while poly I:C and anti-CD40 caused CD80 upregulation on CD11c$^+$ DCs (Mukhopadhaya et al., 2008), eTACs appeared unresponsive to these inflammatory signals, as they failed to upregulate CD80 and were still able to induce tolerance in this setting (Figure 7C, 7D). To determine whether lack of costimulation contributed to eTAC-mediated tolerance induction, we employed an *in vitro* system of CD4-eTAC interaction in which we used an anti-CD28 agonist. Naïve BDC2.5 T cells were stimulated by either AdBDC APCs, or by p31-pulsed WT APCs (Figure S6G). Similar to *in vivo* observations, BDC2.5 T cells became unresponsive to secondary antigen exposure following eTAC interaction, while BDC2.5 T cells stimulated by bulk APCs were able to mount a strong secondary IFN-γ response (Figure 7E). Importantly, provision of exogenous costimulation with anti-CD28 caused a partial reversion of the observed anergy in AdBDC cultures, suggesting that lack of CD28 costimulatory signaling during eTAC interaction with antigen-specific T cells contributes to the mechanism of eTAC-mediated antigen unresponsiveness. Given the high expression of MHC II by eTACs relative to other common APC populations (Figure 7F), we also investigated the contribution of strong TCR signaling to the induction of tolerance. We found that the addition of MHC II blocking antibodies to AdBDC cultures could attenuate the peptide:MHC signal delivered by eTACs, as evidenced by reduced cell cycling (Figure S6H), and result in increased antigen responsiveness among BDC2.5 T cells that had diluted CFSE (Figure 7G). Together, these

results suggest that induction of $CD4^+$ T cell tolerance by eTACs involves a combination of factors that include the delivery of a strong TCR stimulus in the absence of effective costimulation.

Finally, to further address the mechanism of BDC2.5 T cell tolerance and unresponsiveness following interactions with eTACs, we examined signaling events downstream of TCR ligation in BDC2.5 T cells following eTAC-driven tolerance induction. BDC2.5 T cells that had encountered eTACs expressing cognate antigen in lymphoreplete AdBDC mice were severely impaired in their ability to increase calcium in response to TCR stimulus (Figure 7H), and were also unable to initiate TCR signaling through the parallel Ras-MAPK pathway as evidenced by impaired ERK phosphorylation (Figure 7I). These results demonstrate that eTAC-tolerized T cells have impaired TCR signaling, at least affecting events downstream of phospholipase C gamma-1 (PLCg1) activation. These results suggest that eTAC interaction induces robust functional inactivation and antigen unresponsiveness of autoreactive T cells that is highly resistant to conversion from tolerance to immunogenicity.

Discussion

The recent description of *Aire*-expressing cells and ectopic TSA transcription in the periphery has raised the important question of whether intrinsic peripheral self-antigen expression can directly prevent autoimmune disease. Previous descriptions of putatively tolerogenic TSA-expressing populations have focused on deletional tolerance of $CD8^+$ T cells (Gardner et al., 2008; Lee et al., 2007; Nichols et al., 2007), but given widespread MHC class I expression, it was not clear whether this represented a unique feature of these populations or was merely a byproduct of previously unappreciated antigen expression in non-professional APCs. Further, the presence, identity, and ontogeny of *Aire*-expressing populations in the secondary lymphoid organs, and the identity of human eTAC equivalents, have remained unclear. Here we show that mouse and human secondary lymphoid organs contain similar populations of discrete extrathymic *Aire*-expressing cells, that such cells represent a novel bone marrow-derived population of APCs, and that eTACs play a unique role among peripheral TSA-expressing populations by interacting with $CD4^+$ T cells. Further, such interactions promote robust, stable T cell tolerance and prevent progression of autoimmune diabetes.

Our investigation into the origin of eTACs led us to the unexpected conclusion that eTACs are in fact not a stromal population as suggested previously, but are rather bone marrow-derived. The lack of high expression of CD45 and APC markers such as CD11c among cells labeled with the Adig reporter, combined with evidence of radioresistance in adoptive transfer experiments with cognate T cells, had originally indicated that at least some *Aire*-expressing cells in the peripheral lymphoid tissues were radioresistant stromal cells, although initial experiments had also shown that peripheral *Aire*-expressing cells could develop from the bone marrow (Gardner et al., 2008). A comparison of the relative induction of cognate T cell proliferation in reciprocal Adig chimeras in which *Aire*-driven antigen was restricted to either the radioresistant or bone marrow-derived compartment showed that the bone-marrow restricted condition most closely replicated initial observations in unmanipulated Adig mice (Gardner et al., 2008). Further analysis of bone marrow chimeras made with both the Adig and AdBDC reporters of *Aire* expression revealed that the bone marrow compartment was the primary source of *Aire*-driven GFP in these mice, demonstrating that eTACs are bone marrow-derived, and that a degree of radioresistance by eTACs explains their detection in the radioresistant compartment. The possibility also remains that authentic radioresistant stromal cell types express low amounts of Aire and explain our detection of *Aire*-driven antigen in this compartment, but $CD45^{lo}$

MHCII^{hi} CD80^{lo} CD86^{lo} EpCAM^{hi} eTACs appear to be the primary source of Aire in the periphery, and the use of an improved eTAC gating strategy allowed us to identify equivalent amounts of *Aire* expression among sorted peripheral eTACs and Aire^{+} mTECs from the thymus.

Identification of the bone marrow origin of eTACs led to the question of their relationship to other APC populations. Here we have shown that eTACs express low CD45, consistent with their development from the bone marrow. We also identified low CD11c expression in eTACs, as reported in peripheral human lymph nodes (Poliani et al., 2010). Furthermore, we found that eTACs and conventional DCs expressed equivalent amounts of the recently identified transcription factor Zbtb46 (Satpathy et al., 2012), which suggests that eTACs develop through the committed classical DC precursor. Nevertheless, a comparison of surface marker expression between eTACs and conventional DCs shows that while eTACs have a homogenous flow cytometry profile with respect to the markers investigated, they do not clearly fall into any previously identified subset of DCs, supporting the conclusion that eTACs are a distinct and previously undescribed population of APCs.

Consistent with their identity as a distinct professional APC population, we observed that eTACs in transgenic AdBDC mice drove extensive proliferation of cognate T cells. Importantly, direct antigen presentation by eTACs, rather than antigen handoff, was sufficient to induce robust CD4^{+} T cell proliferation, which led to tolerance among CD4^{+} BDC2.5 T cells in a SCID setting. While both functional inactivation of effectors and enrichment of Treg cells may promote such tolerance, it appears that functional inactivation alone following eTAC:T cell interactions is sufficient to prevent autoimmunity, as BDC2.5 FoxP3-DTR^{+} T cells depleted of Treg cells remain unable to transfer disease into AdBDC SCID recipients. Also, eTAC-experienced BDC2.5 T cells were unable to transfer disease serially in *cis* into secondary lymphopenic hosts, and failed to suppress adoptive transfer of disease by other naïve BDC2.5 T cells in *trans*.

Consistently, tolerized BDC2.5 T cells have impaired signaling TCR signaling leading to both the calcium and Ras-MAPK pathways. The precise site of defective signaling likely involves phospholipase C-g1 (PLCg1) activation or upstream events. Biochemical characterization of the site of defective signaling is challenging due to the small number of antigen specific unresponsive cells and will require further study. However, the origin of this impaired signaling is not likely simply attributable to high PD-1 expression since co-ligation of PD-1 with the TCR is required for inhibition of TCR signaling (Chemnitz et al., 2004). Such antigen unresponsiveness might result from incomplete signaling events through T cells undergoing tolerance induction, such as the delivery of antigen in the absence of costimulatory signals in clonal anergy, but is also observed in conditions of repeated antigen exposure including chronic viral infections, where costimulatory pathways are not specifically impaired (Frebel et al., 2010). While eTACs are incompetent to deliver a full signal through the CD28 costimulatory pathway, persistent self-antigen presentation by eTACs and high MHC II expression may also contribute to their tolerance induction through an exhaustion-like pathway of acquired antigen unresponsiveness in which costimulatory signaling is not a major factor in tolerance induction (Singh et al., 2007). However, the inactivation of Erk signaling we observed in eTAC-tolerized cells was more associated with clonal anergy than exhaustion or adaptive tolerance in a biochemical comparison of models for the two states (Chiodetti et al., 2006). Taken together, our results indicate that the primary mechanism of eTAC-mediated disease prevention in this model is recessive—via functional anergy of effectors as opposed to enrichment of Treg cells.

Our results also suggest that eTACs may have uniquely pro-tolerogenic capabilities. In support of this, targeting of a BDC mimetope peptide to another putative tolerogenic APC

population, DEC205$^+$ DCs, induces proliferation of adoptively transferred BDC2.5 T cells similar to that seen in AdBDC recipients, but fails to protect from adoptively transferred diabetes. While the lack of tolerance by DEC1040 was surprising given the established role for immature DEC205$^+$ DCs in tolerance induction (Bonifaz et al., 2002; Mukhopadhaya et al., 2008), DCs from NOD mice may have impaired tolerance (Hamilton-Williams et al., 2009), and prior studies of DEC205$^+$ DCs have focused on tolerance induction of CD8$^+$ T cells. Also, the lymphopenia in SCID mice may override tolerogenic DEC205$^+$ DC antigen presentation, as peripheral antigen display can convert from tolerogenic to immunogenic in the context of lymphopenia (King et al., 2004). It should also be mentioned that delivery of antigen via anti-DEC1040 and via the *Aire* promoter may differ in the dose and length of antigen exposure, which could affect the differential tolerance induction by DEC205$^+$ DCs and eTACs. However, our DEC1040 experiments suggest that eTAC-induced tolerance is not simply a result of the presence of cognate antigen in our disease model, but instead likely depends on additional antigen presentation qualities of eTACs. Indeed, T cell tolerance induced upon eTAC encounter appears insensitive to the perturbations that mitigate many other characterized forms of peripheral tolerance. For example, it is striking that self-antigen expression in eTACs prevents autoimmunity even in lymphopenic SCID mice, and that CD40 and toll-like receptor (TLR) stimuli do not revert eTAC-induced tolerance, in contrast to studies with conventional DC-targeted antigens (Mukhopadhaya et al., 2008). Together these findings suggest that self-antigen expression in eTACs induces a remarkably robust T cell tolerance that is highly resistant to conversion from tolerance to immunogenicity.

Further, these findings distinguish eTACs among putative TSA-expressing peripheral populations in the secondary lymphoid organs. While expression of individual TSA genes has been reported in fibroblastic reticular cells and lymphatic endothelium, these populations do not express *Aire* (Cohen et al., 2010; Fletcher et al., 2010; Lee et al., 2007; Nichols et al., 2007), and while other transcriptional regulators such as Deaf1 may fulfill this same function (Yip et al., 2009), the role of any such factor(s) has not yet been linked to TSA expression in a specific population or to the promotion of immunologic tolerance. Further, while the identification of individual candidate TSA genes expressed in such populations may represent genuine antigen production for the sake of immune education, enrichment for a broad range of ectopically expressed TSA genes appears unique to eTACs (Gardner et al., 2008). This provides an appealing model for complementary tolerance induction to self-reactive T cells that evade adequate negative selection in the thymus, and the fact that such TSA-expressing eTACs can induce tolerance among both CD4$^+$ and CD8$^+$ T cells further supports a broad role for this population in peripheral tolerance.

Together these results demonstrate that eTACs are a distinct type of bone marrow-derived APC, and that targeted antigen expression in eTACs induces robust peripheral self-tolerance through the induction of antigen unresponsiveness. The ability of eTACs to confer such tolerance in secondary hosts represents an attractive therapeutic application for this population in the re-establishment of immune tolerance in both autoimmunity and transplantation. Finally, our findings that eTACs are a distinct bone marrow-derived population from the classical DC lineage should facilitate the identification and development of *in vitro* differentiation and expansion conditions that will make therapeutic eTAC transfers feasible for the induction of antigen-specific immune tolerance.

Experimental Procedures

Transgene construction, BAC recombineering, and purification

Aire-driven BDC2.5 peptide (AdBDC) transgenic mice were generated by standard cloning methods using a bacterial artificial chromosome (BAC) recombineering and transgenesis

strategy. Full description of primers, reagents, and recombineering strategy can be found in Supplemental Experimental Procedures.

Mice and genotyping

AdBDC and Adig transgenic NOD mice were screened by real-time PCR for GFP, and were maintained in heterozygosity for all experiments. Additional information on mouse strains and genotyping appears in the Supplemental Experimental Procedures. All mice were maintained in microisolator cages and treated in accordance with NIH and American Association of Laboratory Animal Care standards, and consistent with the animal care and use regulations of the University of California, San Francisco.

Flow Cytometry and Cell Sorting

All flow cytometry antibodies were purchased from BD Pharmingen, eBioscience, Invitrogen, or Southern Biotech with the exception of anti-CD16/32 (clone 2.4G2), which was purified by the UCSF hybridoma core. Lymphocytes for flow cytometry were prepared by mashing thymi, lymph nodes, or spleens, filtering through a 70μm cell-strainer, ACK lysis of red blood cells (spleen only), counting by trypan blue exclusion, resuspending in Fc block (2.4G2), and staining in FACS buffer.

eTAC, mTEC, DC and macrophage populations were isolated by digestion in a mixture of collagenase, dispase, and DNase followed by Percoll density centrifugation, as described by Gardner et al. (2008). Populations were identified as follows: cDCs ($DAPI^-$, $CD45^{hi}$, $MHCII^+$, $CD11c^{hi}$), Aire+ mTECs ($DAPI^-$, $CD11c^-$, $EpCAM^+$, $CD45^-$, $MHCII^+$, Aire-GFP^+), B cells (FSC vs. SSC, $CD19^+$, $CD45^+$, $CD11c^-$), $CD4^+$ T cells (FSC vs. SSC, $CD4^+$, $CD45^+$, $CD11c^-$), macrophages (FSC vs. SSC, F4/80+, CD45+). Cells were analyzed with a BD LSRII cytometer and sorted on a BD FACSAria III cell sorter. Tetramer, Foxp3, phospho-Erk, Calcium FACS assays, and mRNA transcript analysis by qPCR were performed as described in Supplemental Experimental Procedures.

Immunofluorescent staining and histology

Immunofluorescent staining was conducted as described in the Supplemental Experimental Procedures. To visualize cytosolic GFP in AdBDC mice, tissues were fixed in 1.5% PFA followed TSA amplification of GFP staining (Perkin Elmer). For human sections, formalin-fixed, paraffin-embedded sections obtained from the JDRF nPOD project were processed for antigen retrieval prior to TSA amplification of AIRE signal.

Reciprocal bone marrow chimeras

WT and Aire-GFP reporter mice (Adig for *8.3* adoptive transfers, AdBDC mice for the displayed Aire-GFP plots) were used as donors and/or recipients to generate chimeric mice to restrict transgene expression to the bone marrow, radioresistant host, neither, or both compartments. Recipient mice received two irradiation cycles totaling 1300 rads (900 rads, 400 rads), with at least 3 hours between doses. Donor bone marrow was harvested, depleted of T cells as described previously (Gardner et al., 2008), and injected i.v. at 1×10^7 cells per host. Mice were harvested after at least 8 weeks of reconstitution.

Purification, CFSE-labeling, and adoptive and serial transfers of T cells

For adoptive transfer of naïve, CD25-depleted, CD4-enriched T cells, spleen and non-pancreatic lymph nodes were harvested from nondiabetic donors, pooled by group, ACK-lysed and counted. Cells were CD25-depleted with anti-CD25 (7D4) and CD4-enriched using a Mouse $CD4^+$ Negative Selection Kit (StemCell). Aliquots at each step were analyzed to confirm purity. Purified cells were pooled in a ~1:1 ratio of BDC2.5 T cells to

polyclonal $CD4^+$ T cells, labeled in 2.5μM CFSE (Invitrogen) for proliferation experiments, and injected intravenously (IV) at 1–2 × 10^6 cells/mouse in HBSS. *8.3* $CD8^+$ T cells were prepared similarly using a Robosep $CD8^+$ T cell Negative Selection kit. For adoptive transfer of diabetes, 2 × 10^5 unlabeled cells/mouse were injected IV. Serial co-transfer of T cells was performed by harvesting non-pancreatic lymph nodes and spleen from SCID and AdBDC SCID primary recipients at day 10. Cells were CD4-purified as described above, and injected to secondary SCID hosts either alone or mixed 1:1 with naïve BDC2.5 T cells at 2 × 10^5 cells/recipient.

In vitro tolerance assay

Naïve T cells were prepared and mixed with Percoll-enriched APCs isolated from WT or AdBDC mice by density centrifugation as described previously (Gardner et al., 2008). 1 × 10^5 naïve BDC2.5 T cells were mixed with 1×10^6 APCs in 24-well plates, and incubated for 7 days at 37° C in complete DMEM media. Acetylated p31 peptide (YVRPLWVRME, GenScript) ((Judkowski et al., 2001) was added to control activating conditions at 1 ug/mL. Anti-CD28 (PV-1) was added to indicated cultures at 0.5 ug/mL. Stimulated T cells were isolated by Robosep CD4 enrichment, rested overnight in complete DMEM media, and analyzed for IFN-γ production to a second stimulation with 1 ug/mL p31 and bulk Thy1.2+ splenocytes (described for CFA immunization assay). For MHC II blocking experiments, anti-I-A^{g7} (clone AG2.42.7, provided by E. Unanue) was used at 10 ug/mL. 2 × 10^4 naïve BDC2.5 T cells were mixed with 2.5 × 10^4 APCs in flat-bottom 96-well plates, and incubated for 7 days at 37° C in complete DMEM media before being rested overnight and restimulated with PMA and Ionomycin.

Statistical Analysis

Statistical analysis of data was performed with Microsoft Excel 2003 and GraphPad Prism 4.0. Statistical comparisons were made using paired t-tests and a two-tailed 95% confidence interval.

Supplementary Material

Refer to Web version on PubMed Central for supplementary material.

Acknowledgments

We thank M. Cheng for critical reading of the manuscript; J. Esensten, J. Bluestone, Q. Tang, H. van Santen, P. Peterson, H. Scott, E. Unanue, D. Mathis and C. Benoist for reagents and mice, and N. Killeen and the UCSF Transgenic Core for help generating transgenic mice. Supported by the US National Institutes of Health AI035297 (M.S.A), DK59958 for core support, the Helmsley Charitable Trust (M.S.A, T.C.M), the American Diabetes Association (J.M.G.), the UCSF Medical Scientist Training Program (J.M.G.), the UCSF Department of Surgery (J.M.G.) and the intramural research program of the National Institute of Diabetes and Digestive and Kidney Diseases, NIH (J.P. and K.T.). This research was performed with the support of the Network for Pancreatic Organ Donors with Diabetes (nPOD), a collaborative type 1 diabetes research project sponsored by the Juvenile Diabetes Research Foundation International (JDRF). Organ Procurement Organizations (OPO) partnering with nPOD to provide research resources are listed at www.jdrfnpod.org/our-partners.php.

References

Anderson MS, Venanzi ES, Chen Z, Berzins SP, Benoist C, Mathis D. The cellular mechanism of Aire control of T cell tolerance. Immunity. 2005; 23:227–239. [PubMed: 16111640]

Anderson MS, Venanzi ES, Klein L, Chen Z, Berzins SP, Turley SJ, von Boehmer H, Bronson R, Dierich A, Benoist C, et al. Projection of an immunological self shadow within the thymus by the aire protein. Science (New York, NY). 2002; 298:1395–1401.

Bettini M, Szymczak-Workman AL, Forbes K, Castellaw AH, Selby M, Pan X, Drake CG, Korman AJ, Vignali DA. Cutting edge: accelerated autoimmune diabetes in the absence of LAG-3. Journal of immunology (Baltimore, Md : 1950). 2011; 187:3493–3498.

Bonifaz L, Bonnyay D, Mahnke K, Rivera M, Nussenzweig MC, Steinman RM. Efficient targeting of protein antigen to the dendritic cell receptor DEC-205 in the steady state leads to antigen presentation on major histocompatibility complex class I products and peripheral CD8+ T cell tolerance. The Journal of experimental medicine. 2002; 196:1627–1638. [PubMed: 12486105]

Chemnitz JM, Parry RV, Nichols KE, June CH, Riley JL. SHP-1 and SHP-2 associate with immunoreceptor tyrosine-based switch motif of programmed death 1 upon primary human T cell stimulation, but only receptor ligation prevents T cell activation. Journal of immunology (Baltimore, Md : 1950). 2004; 173:945–954.

Chiodetti L, Choi S, Barber DL, Schwartz RH. Adaptive tolerance and clonal anergy are distinct biochemical states. Journal of immunology (Baltimore, Md : 1950). 2006; 176:2279–2291.

Cohen JN, Guidi CJ, Tewalt EF, Qiao H, Rouhani SJ, Ruddell A, Farr AG, Tung KS, Engelhard VH. Lymph node-resident lymphatic endothelial cells mediate peripheral tolerance via Aire-independent direct antigen presentation. The Journal of experimental medicine. 2010; 207:681–688. [PubMed: 20308365]

Derbinski J, Schulte A, Kyewski B, Klein L. Promiscuous gene expression in medullary thymic epithelial cells mirrors the peripheral self. Nature immunology. 2001; 2:1032–1039. [PubMed: 11600886]

Feuerer M, Shen Y, Littman DR, Benoist C, Mathis D. How punctual ablation of regulatory T cells unleashes an autoimmune lesion within the pancreatic islets. Immunity. 2009; 31:654–664. [PubMed: 19818653]

Fletcher AL, Lukacs-Kornek V, Reynoso ED, Pinner SE, Bellemare-Pelletier A, Curry MS, Collier AR, Boyd RL, Turley SJ. Lymph node fibroblastic reticular cells directly present peripheral tissue antigen under steady-state and inflammatory conditions. The Journal of experimental medicine. 2010; 207:689–697. [PubMed: 20308362]

Frebel H, Richter K, Oxenius A. How chronic viral infections impact on antigen-specific T-cell responses. European journal of immunology. 2010; 40:654–663. [PubMed: 20077405]

Gardner JM, Devoss JJ, Friedman RS, Wong DJ, Tan YX, Zhou X, Johannes KP, Su MA, Chang HY, Krummel MF, et al. Deletional tolerance mediated by extrathymic Aire-expressing cells. Science (New York, NY). 2008; 321:843–847.

Halonen M, Pelto-Huikko M, Eskelin P, Peltonen L, Ulmanen I, Kolmer M. Subcellular location and expression pattern of autoimmune regulator (Aire), the mouse orthologue for human gene defective in autoimmune polyendocrinopathy candidiasis ectodermal dystrophy (APECED). The journal of histochemistry and cytochemistry : official journal of the Histochemistry Society. 2001; 49:197–208. [PubMed: 11156688]

Hamilton-Williams EE, Martinez X, Clark J, Howlett S, Hunter KM, Rainbow DB, Wen L, Shlomchik MJ, Katz JD, Beilhack GF, et al. Expression of diabetes-associated genes by dendritic cells and CD4 T cells drives the loss of tolerance in nonobese diabetic mice. Journal of immunology (Baltimore, Md : 1950). 2009; 183:1533–1541.

Harding FA, McArthur JG, Gross JA, Raulet DH, Allison JP. CD28-mediated signalling co-stimulates murine T cells and prevents induction of anergy in T-cell clones. Nature. 1992; 356:607–609. [PubMed: 1313950]

Heino M, Peterson P, Sillanpaa N, Guerin S, Wu L, Anderson G, Scott HS, Antonarakis SE, Kudoh J, Shimizu N, et al. RNA and protein expression of the murine autoimmune regulator gene (Aire) in normal, RelB-deficient and in NOD mouse. European journal of immunology. 2000; 30:1884–1893. [PubMed: 10940877]

Hubert FX, Kinkel SA, Webster KE, Cannon P, Crewther PE, Proeitto AI, Wu L, Heath WR, Scott HS. A specific anti-Aire antibody reveals aire expression is restricted to medullary thymic epithelial cells and not expressed in periphery. Journal of immunology (Baltimore, Md : 1950). 2008; 180:3824–3832.

Judkowski V, Pinilla C, Schroder K, Tucker L, Sarvetnick N, Wilson DB. Identification of MHC class II-restricted peptide ligands, including a glutamic acid decarboxylase 65 sequence, that stimulate

diabetogenic T cells from transgenic BDC2.5 nonobese diabetic mice. Journal of immunology (Baltimore, Md : 1950). 2001; 166:908–917.

Katz JD, Wang B, Haskins K, Benoist C, Mathis D. Following a diabetogenic T cell from genesis through pathogenesis. Cell. 1993; 74:1089–1100. [PubMed: 8402882]

King C, Ilic A, Koelsch K, Sarvetnick N. Homeostatic expansion of T cells during immune insufficiency generates autoimmunity. Cell. 2004; 117:265–277. [PubMed: 15084263]

Lathrop SK, Huddleston CA, Dullforce PA, Montfort MJ, Weinberg AD, Parker DC. A signal through OX40 (CD134) allows anergic, autoreactive T cells to acquire effector cell functions. Journal of immunology (Baltimore, Md : 1950). 2004; 172:6735–6743.

Lee JW, Epardaud M, Sun J, Becker JE, Cheng AC, Yonekura AR, Heath JK, Turley SJ. Peripheral antigen display by lymph node stroma promotes T cell tolerance to intestinal self. Nature immunology. 2007; 8:181–190. [PubMed: 17195844]

Lukacs-Kornek V, Malhotra D, Fletcher AL, Acton SE, Elpek KG, Tayalia P, Collier AR, Turley SJ. Regulated release of nitric oxide by nonhematopoietic stroma controls expansion of the activated T cell pool in lymph nodes. Nature immunology. 2011; 12:1096–1104. [PubMed: 21926986]

Malhotra D, Fletcher AL, Astarita J, Lukacs-Kornek V, Tayalia P, Gonzalez SF, Elpek KG, Chang SK, Knoblich K, Hemler ME, et al. Transcriptional profiling of stroma from inflamed and resting lymph nodes defines immunological hallmarks. Nature immunology. 2012; 13:499–510. [PubMed: 22466668]

Martinez RJ, Zhang N, Thomas SR, Nandiwada SL, Jenkins MK, Binstadt BA, Mueller DL. Arthritogenic self-reactive CD4+ T cells acquire an FR4hiCD73hi anergic state in the presence of Foxp3+ regulatory T cells. Journal of immunology (Baltimore, Md : 1950). 2012; 188:170–181.

Metzger TC, Anderson MS. Control of central and peripheral tolerance by Aire. Immunological reviews. 2011; 241:89–103. [PubMed: 21488892]

Mukhopadhaya A, Hanafusa T, Jarchum I, Chen YG, Iwai Y, Serreze DV, Steinman RM, Tarbell KV, DiLorenzo TP. Selective delivery of beta cell antigen to dendritic cells in vivo leads to deletion and tolerance of autoreactive CD8+ T cells in NOD mice. Proceedings of the National Academy of Sciences of the United States of America. 2008; 105:6374–6379. [PubMed: 18430797]

Nagamine K, Peterson P, Scott HS, Kudoh J, Minoshima S, Heino M, Krohn KJ, Lalioti MD, Mullis PE, Antonarakis SE, et al. Positional cloning of the APECED gene. Nature genetics. 1997; 17:393–398. [PubMed: 9398839]

Nichols LA, Chen Y, Colella TA, Bennett CL, Clausen BE, Engelhard VH. Deletional self-tolerance to a melanocyte/melanoma antigen derived from tyrosinase is mediated by a radio-resistant cell in peripheral and mesenteric lymph nodes. Journal of immunology (Baltimore, Md : 1950). 2007; 179:993–1003.

Poliani PL, Kisand K, Marrella V, Ravanini M, Notarangelo LD, Villa A, Peterson P, Facchetti F. Human peripheral lymphoid tissues contain autoimmune regulator-expressing dendritic cells. The American journal of pathology. 2010; 176:1104–1112. [PubMed: 20093495]

Satpathy AT, Kc W, Albring JC, Edelson BT, Kretzer NM, Bhattacharya D, Murphy TL, Murphy KM. Zbtb46 expression distinguishes classical dendritic cells and their committed progenitors from other immune lineages. The Journal of experimental medicine. 2012; 209:1135–1152. [PubMed: 22615127]

Shum AK, DeVoss J, Tan CL, Hou Y, Johannes K, O'Gorman CS, Jones KD, Sochett EB, Fong L, Anderson MS. Identification of an autoantigen demonstrates a link between interstitial lung disease and a defect in central tolerance. Science translational medicine. 2009; 1:9ra20.

Singh NJ, Cox M, Schwartz RH. TLR ligands differentially modulate T cell responses to acute and chronic antigen presentation. Journal of immunology (Baltimore, Md : 1950). 2007; 179:7999–8008.

Stadinski BD, Delong T, Reisdorph N, Reisdorph R, Powell RL, Armstrong M, Piganelli JD, Barbour G, Bradley B, Crawford F, et al. Chromogranin A is an autoantigen in type 1 diabetes. Nature immunology. 2010; 11:225–231. [PubMed: 20139986]

Su MA, Giang K, Zumer K, Jiang H, Oven I, Rinn JL, Devoss JJ, Johannes KP, Lu W, Gardner J, et al. Mechanisms of an autoimmunity syndrome in mice caused by a dominant mutation in Aire. The Journal of clinical investigation. 2008; 118:1712–1726. [PubMed: 18414681]

van Santen HM, Benoist C, Mathis D. Number of T reg cells that differentiate does not increase upon encounter of agonist ligand on thymic epithelial cells. The Journal of experimental medicine. 2004; 200:1221–1230. [PubMed: 15534371]

Yip L, Su L, Sheng D, Chang P, Atkinson M, Czesak M, Albert PR, Collier AR, Turley SJ, Fathman CG, et al. Deaf1 isoforms control the expression of genes encoding peripheral tissue antigens in the pancreatic lymph nodes during type 1 diabetes. Nature immunology. 2009; 10:1026–1033. [PubMed: 19668219]

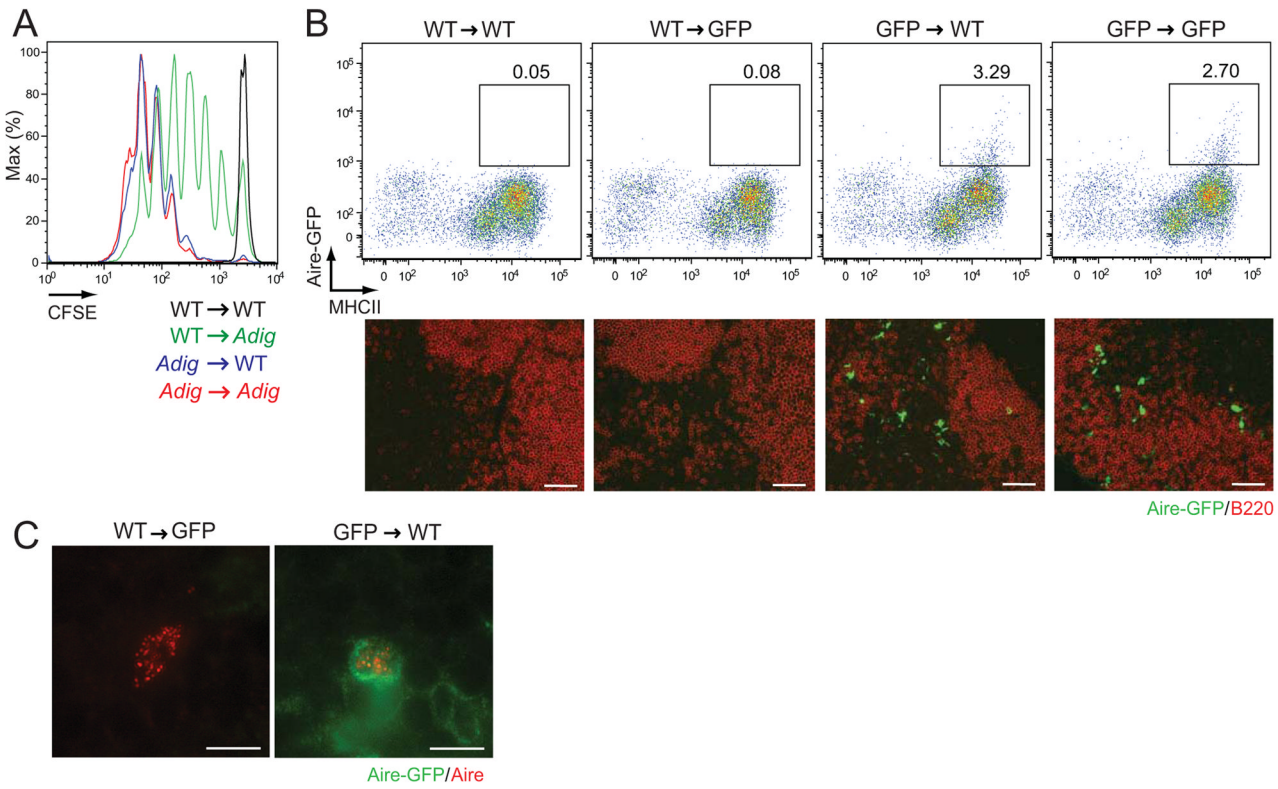

Figure 1.

eTACs are bone marrow-derived. (**A**) CFSE dilution among Thy1.1-labeled *8.3* T cells in non-pancreatic lymph nodes three days after adoptive transfer into reciprocal Adig chimeras. Representative of two independent sets of chimeras. (**B**) Top: flow cytometric analysis of peripheral lymphoid organs from reciprocal bone marrow chimeras, made using WT and Aire-GFP reporter mice (performed in three independent experiments with Adig or AdBDC mice, see Fig. 4). Pre-gated on $DAPI^{-}$, $CD45^{lo}$ events. Bottom: Immunofluorescent images of lymph node sections from reciprocal chimeras, with Aire-driven GFP (green) and B220 (red) staining. Scale bars = 50 μm. Performed in three independent experiments with Adig or AdBDC mice, see Fig. 4. (**C**) Immunofluorescent detection of Aire protein (red) and Aire-driven GFP (green) in chimeras from (**B**). Scale bars = 7 μm, see also Figure S1.

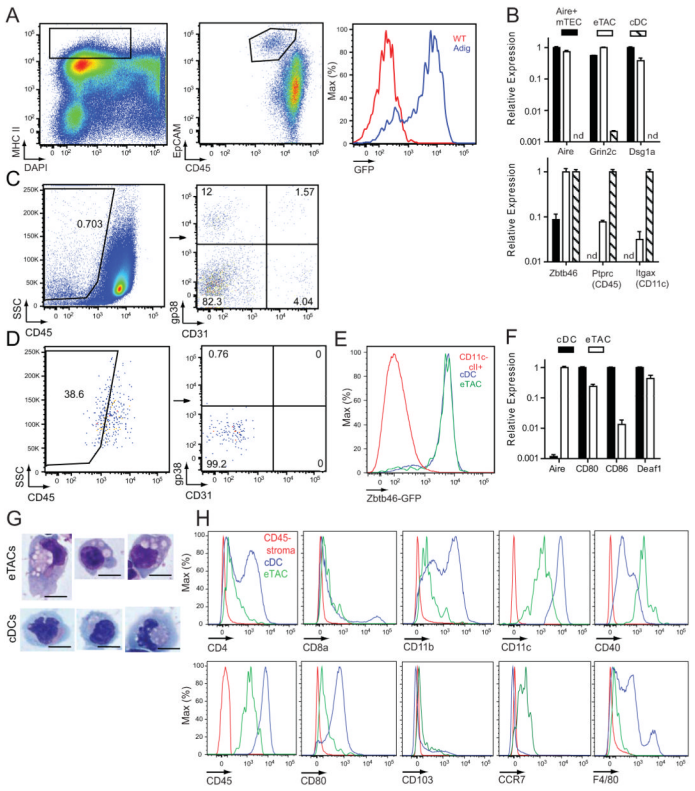

Figure 2.

eTACs are a distinct type of antigen presenting cell. (**A**) Identification of splenic eTACs without a GFP reporter. MHCII^{+} DAPI^{-} events are shown on a CD45 vs. EpCAM plot, and histograms of GFP expression are shown among a distinct EpCAM^{+} CD45^{lo} population. (**B**) Quantitative PCR results of relative mRNA expression, Mean + SD, standardized to Ppia, in indicated populations. nd = not detected. Results are representative of at least two independent experiments per target. (**C**) Flow cytometric analysis of DAPI-, FSC vs. SSC Percoll light fractions from WT and Aire-GFP spleen. Representative of three independent experiments. (**D**) Back-gating of eTAC events, identified with an equivalent gating strategy to (**A**), onto the stromal cell identification approach shown in (**C**). (**E**) Flow cytometric analysis of spleen tissue from *Zbtb46*-GFP/WT mice showing GFP expression by the indicated populations. n=4 *Zbtb46*-GFP/WT or *Zbtb46*-GFP/GFP mice. (**F**) Additional qPCR analyses of target gene expression by eTACs and cDCs analyzed as in (**B**), mean + SD. (**G**) Giemsa staining of indicated populations from the spleens of Adig donors, cytospun onto slides, and visualized by light microscopy. Representative of two independent experiments. eTACs: FSC vs. SSC, DAPI^{-}, CD45^{lo}, MHCII^{hi}, CD86^{-}, Aire-GFP^{+}. Scale bars = 10 μm. (**H**) Flow cytometric analysis of the indicated markers on eTACs (green), CD45^{-} stromal cells (red), and cDCs (blue). Representative of at least three independent experiments, see also Figure S2.

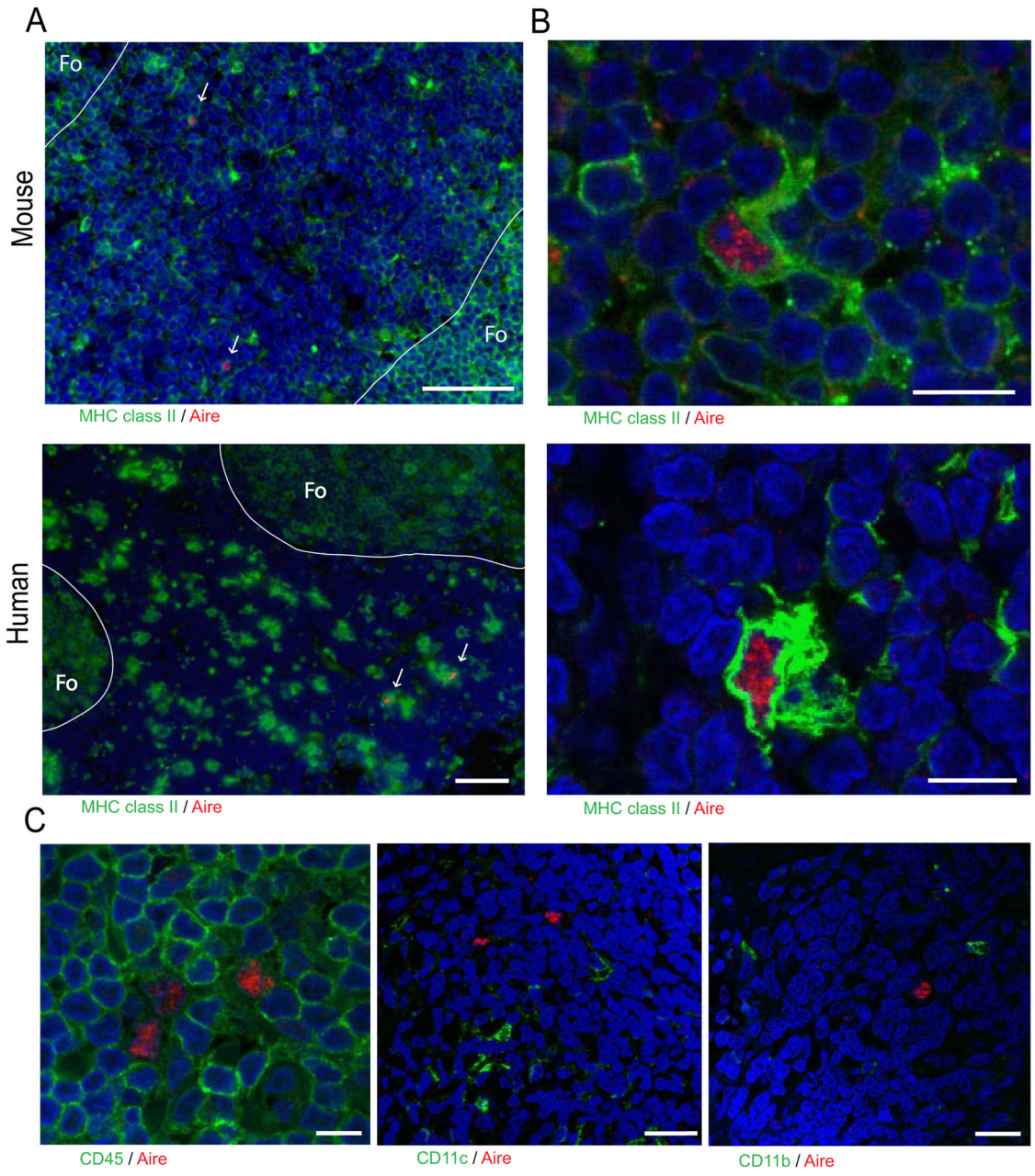

Figure 3.

eTACs are present in human lymph nodes. (**A**) Immunofluorescent staining of eTACs from indicated lymph nodes counterstained with DAPI (blue), showing localization of eTACs to the T cell zone near B cell follicles. Note the rare Aire^{+} MHC II^{+} cells in the T cell zones (arrows). The outline of the follicle (Fo) is highlighted. Scale bar = 50 μm. Four independent experiments were performed with human samples. (**B**) Representative confocal images of eTACs in (**A**) showing nuclear Aire speckling. Scale bar = 10 μm. (**C**) Confocal images of eTACs with Aire (red) and co-staining of CD45 (left, scale bar = 10 μm), CD11c (center, scale bar = 25 μm), and CD11b (right, scale bar = 25 μm). Representative of at least two independent experiments per target, see also Figure S3.

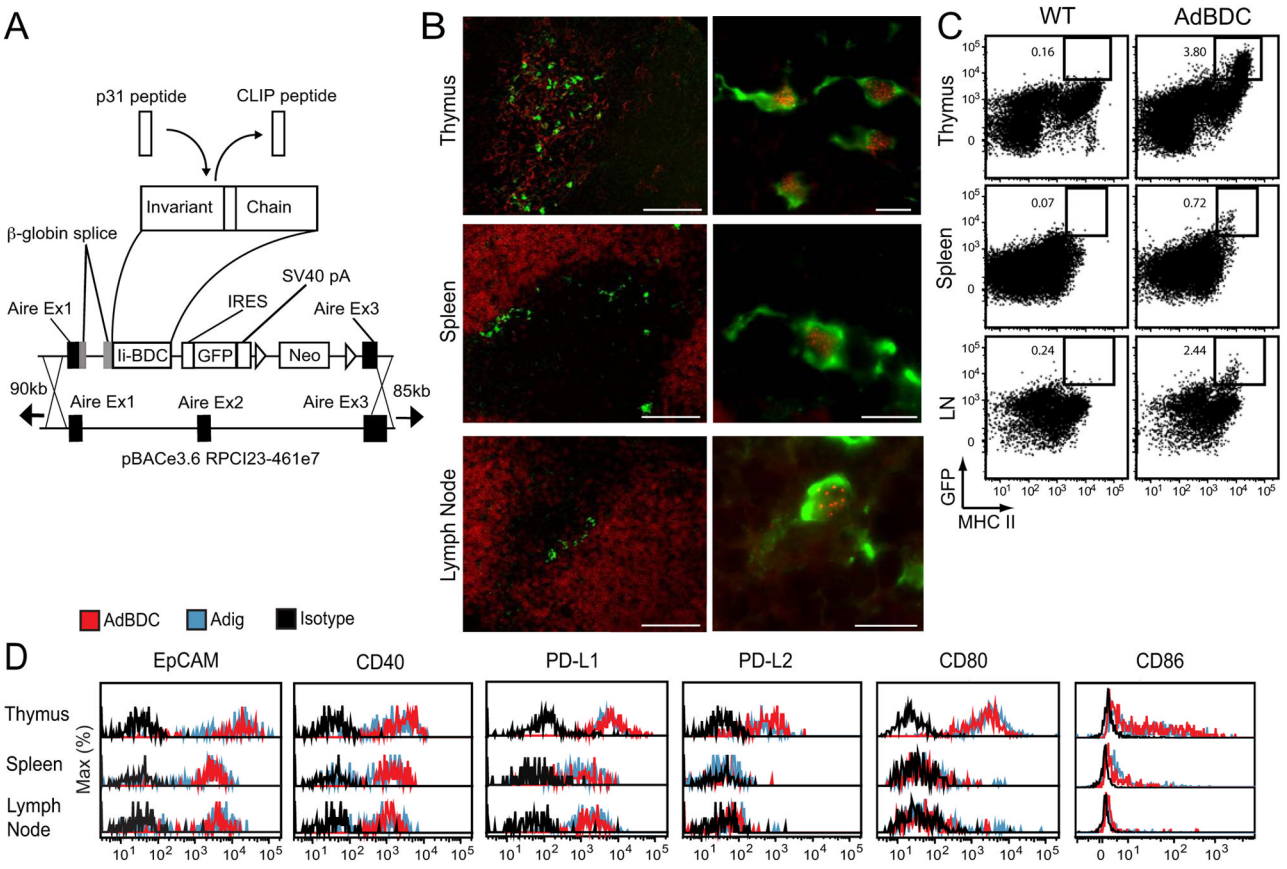

Figure 4.

The AdBDC transgene drives expression of the p31 mimetope peptide in *Aire*-expressing cells. (**A**) Schematic of *Aire*-driven BDC peptide Invariant Chain-GFP construct targeting the bacterial artificial chromosome (BAC) containing the murine *Aire* locus. The MHC class II-associated invariant chain peptide (CLIP) was replaced with the p31 peptide to facilitate its loading into MHC II molecules of *Aire*-expressing cells. (**B**) Immunofluorescent staining of AdBDC tissues with anti-GFP (green; all panels), B220 (red; spleen and lymph node left panels), cytokeratin 5 (red; thymus left panel) and anti-Aire (red, right panels). Representative of at least two independent experiments per analysis. (**C**) Flow cytometric analysis of GFP and MHC II expression from WT and AdBDC NOD tissues (pre-gated on $CD45^{lo}$, $DAPI^{-}$). Representative of multiple independent experiments. (**D**) Flow cytometric analysis of $DAPI^{-}$, $CD45^{lo}$, GFP^{+} populations with isotype control (black), or indicated markers from Adig (blue) and AdBDC (red) mice.

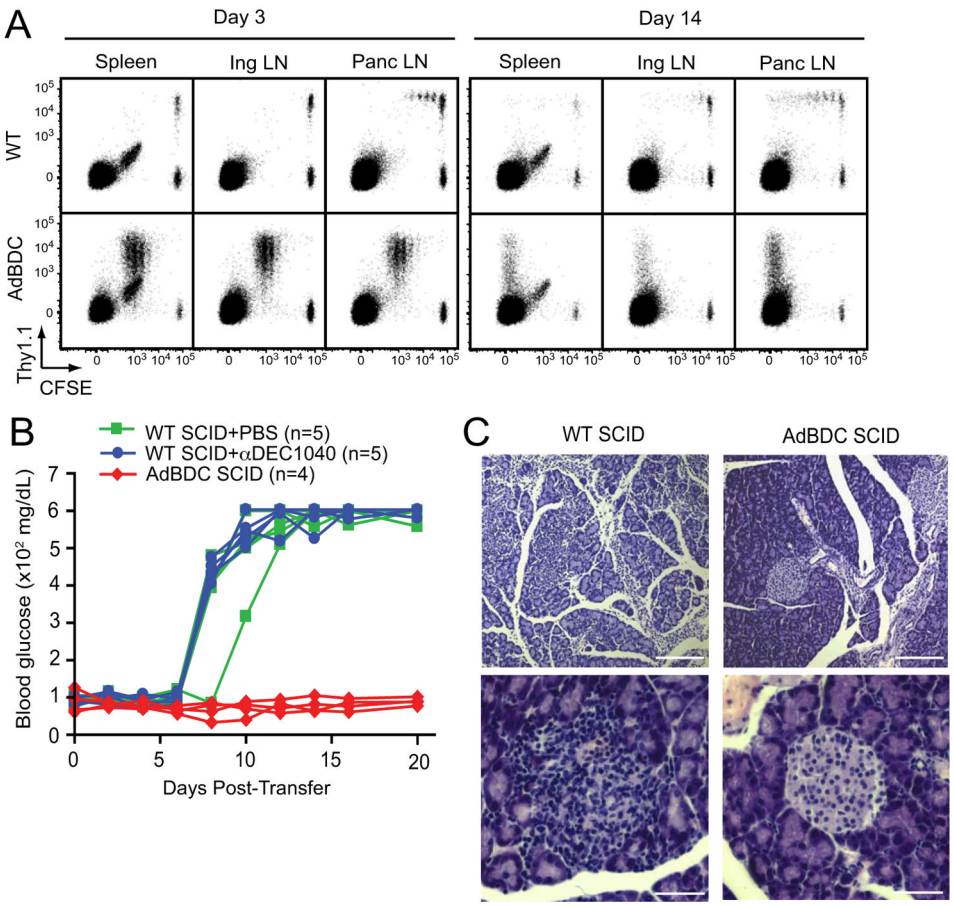

Figure 5.

eTACs in AdBDC mice interact with CD4$^+$ BDC2.5 T cells and prevent induction of autoimmune diabetes in SCID mice. (**A**) Flow cytometric analysis of CD4$^+$ lymphocyte populations in after adoptive co-transfer of CFSE-labeled Thy1.1$^+$ BDC2.5 T cells and Thy1.2$^+$ polyclonal T cells to indicated hosts. Representative of at least three independent experiments. (**B**) Blood sugar values (mg/dl) among indicated mice following adoptive transfer of BDC2.5 T cells. Results are pooled from two independent cohorts. (**C**) Hematoxylin and eosin-stained pancreatic islet histology of indicated adoptive transfer recipients at day 10 post-transfer. Upper panel scale bars = 200 μm, lower panel scale bars = 50 μm. Representative of two independent experiments, see also Figure S4.

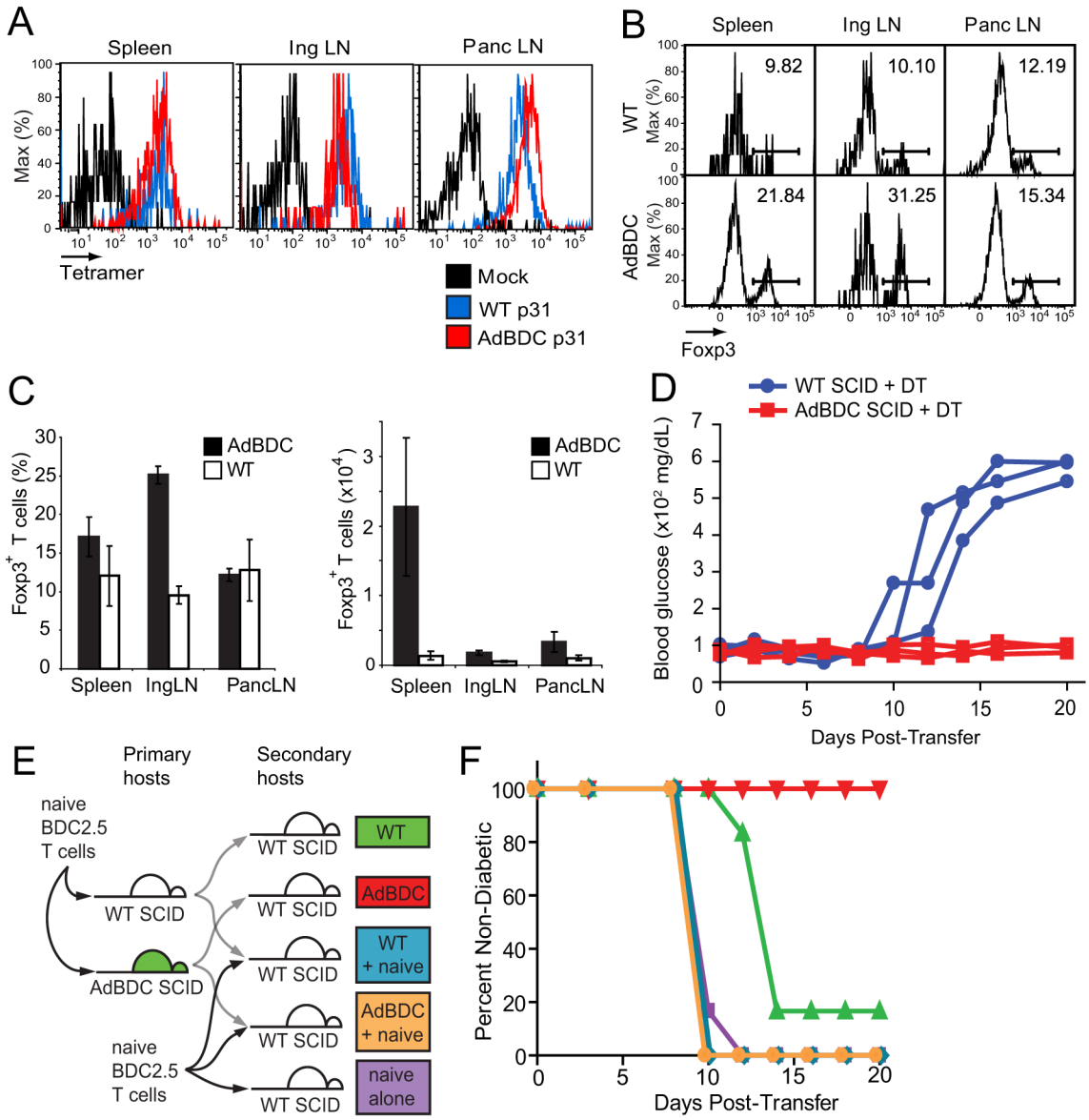

Figure 6.

Regulatory T cells are dispensable for eTAC-induced tolerance. (**A**) Flow cytometric analysis of I-Ag7-p31 tetramer avidity among residual Thy1.1$^+$ BDC2.5 T cells at day 14 post-adoptive transfer into indicated hosts compared with mock I-Ag7-CLIP tetramer (black). (**B**) Foxp3 staining of CD4$^+$ Thy1.1$^+$ BDC2.5 T cells 14 days after adoptive transfer to indicated hosts. (**C**) Quantitation of (**B**) showing percentage of Thy1.1$^+$ CD4$^+$ cells that are Foxp3$^+$ (left) and total number of Foxp3$^+$ cells (right) in indicated recipients, Mean +/− SD. (**D**) Blood sugar values (mg/dl) among DT-treated hosts after adoptive transfer of CD4-enriched, DT-treated BDC2.5 Foxp3-DTR T cells, n=3 per condition. (**E**) Schematic illustration of BDC2.5 serial adoptive transfer strategy. Naive BDC2.5 T cells were transferred into primary hosts; at day 10, lymphocytes were re-harvested, purified, and serially transferred into WT SCID secondary hosts alone or in a 1:1 mixture with fresh, naïve BDC2.5 T cells. (**F**) Diabetes incidence after adoptive transfer among secondary hosts

indicated in (**E**), n=6 per condition, pooled from two independent cohorts, see also Figure S5.

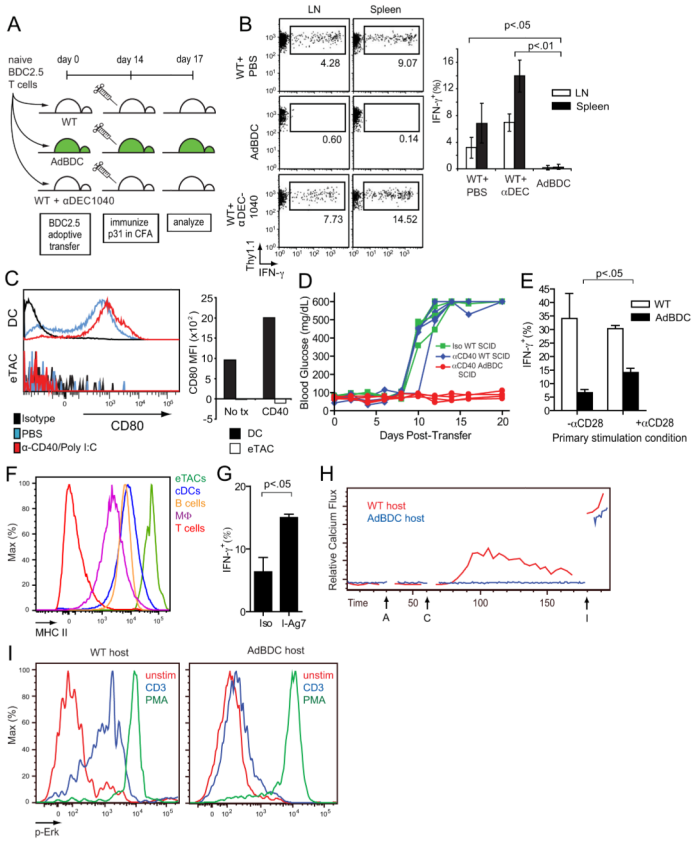

Figure 7.

eTACs induce functional inactivation of cognate T cells by presenting antigen in the absence of costimulation. (**A**) Schematic of p31+CFA immunization protocol to measure recall response of adoptively transferred BDC2.5 T cells. Naïve BDC2.5 T cells were transferred to indicated mice, which were immunized with p31 in complete freund's adjuvant (CFA) 14 days later. IFN-γ production to this second stimulation was assessed *ex vivo* after three days. (**B**) IFN-γ production among $CD4^+$ $Thy1.1^+$ BDC2.5 T cells isolated from mice indicated in (**A**); bar graph shows quantification of pooled data with n=4 for each group, Mean +/− SD. Results are pooled from two independent experiments. (**C**) Representative flow cytometric analysis of CD80 staining in $DAPI^-$, $CD45^+$, $CD11c^+$ DCs and $DAPI^-$, $CD45^{lo}$, $MHCII^+$, GFP^+ eTACs in response to anti-CD40+PolyI:C stimulus; quantification of MFI shifts above isotype levels shown at right. (**D**) Blood sugar values (mg/dL) among anti-CD40+PolyI:C treated hosts after adoptive transfer of naive BDC2.5 T cells, n=4 per condition, pooled from three independent experiments. (**E**) IFN-γ recall responses (% of $CD4^+$ T cells) by CD4-enriched BDC2.5 T cells cultured with AdBDC or p31-pulsed WT primary APCs, and with anti-CD28 where indicated, responding to p31 + APC re-stimulation, Mean + SD. Data was pooled from three independent experiments. (**F**) Representative flow cytometric analysis of MHC II expression among by indicated populations. MΦ = macrophages. (**G**) IFN-γ recall responses by $CD4^+$ $Thy1.1^+$ $CFSE^{lo}$ BDC2.5 T cells following culture with AdBDC APCs and either anti-I-A^{g7} MHC II blocking antibody or isotype, Mean + SD. (**H**) Kinetic plots of relative Calcium signaling over time (seconds) of *ex vivo* BDC2.5 $Thy1.1^+$ T cells recovered from indicated hosts and 14 days post-transfer, as detected by Indo-1 dyes. A - anti-CD3, C - cross-linking secondary, I – ionomycin. Results are representative of three independent experiments. (**I**) Flow cytometric analysis of Erk phosphorylation of rested $Thy1.1^+$ $CD4^+$ T cell populations in

(**H**) after a 2 minute stimulation with anti-CD3 (blue) or PMA (green). Results are representative of three independent experiments, see also Figure S6.